SILICON BASED HYBRID PHOTONIC CRYSTAL WAVEGUIDE WITH DEFECTS FOR DIRECTIONAL COUPLER AND RING RESONATORS

RONALD BIN BAKAR

UNIVERSITI SAINS MALAYSIA

2024

SILICON BASED HYBRID PHOTONIC CRYSTAL WAVEGUIDE WITH DEFECTS FOR DIRECTIONAL COUPLER AND RING RESONATORS

by

RONALD BIN BAKAR

Thesis submitted in fulfilment of the requirements for the degree of Master of Science

May 2024

ACKNOWLEDGEMENT

I would like to thank my supervisor Ts. Dr Wan Maryam Wan Ahmad Kamil for her guidance, tutelage, support, and valuable advice, of which have greatly facilitated towards the completion of this work. Also, I would like to thank my co-supervisor Honorary Prof. Dr. Haslan Abu Hassan, also for his for the guidance, tutelage, support, and valuable advice, even beyond retirement. To both my supervisors, I am forever indebted.

I would also like to thank fellow peers and candidates who have been of great help with guidance and support, I wish you all the best too for your pursuits, current and future. Also, I wish to express my gratitude to my family and friends for their endless support and encouragement, direct and indirect, all of which have been really valuable to me that they are priceless. To everyone, many thanks.

TABLE OF CONTENTS

ACKN	NOWLED	GEMENT	ii
TABL	E OF CO	ONTENTS	iii
LIST	OF FIGU	RES	vi
LIST	OF SYMI	BOLS	xii
LIST	OF ABBI	REVIATIONS	xiii
ABST	RAK		xiv
ABST	RACT		XV
СНАР	TER 1	INTRODUCTION	1
1.1	Chapter (Overview	1
1.2	Backgrou	and of Research	1
1.3	Problem Statement		
1.4	Research Motivation		
1.5	Scope of Simulation		
1.6	Research	Objectives	6
1.7	Thesis O	utline	6
СНАР	TER 2	LITERATURE REVIEW	8
2.1	Chapter (Overview	8
2.2	Backgrou	and of Photonic Band Gap and Photonic Crystals	8
2.3	Base Pho	otonic Crystal Structure	13
	2.3.1	Substrate Materials and Layout	13
	2.3.2	The Gap Map	14
2.4	Photonic	Crystal Defects	15
	2.4.1	Photonic Crystal Slab Waveguide	16
	2.4.2	Directional Coupler for WDM by Line Defects	20
	2.4.3	Cavity Filter for WDM by Point Defects	22

	2.4.4	Hybrid PhC Structures	23
2.5	Simulati	on Methods	24
	2.5.1	Plane-wave Expansion (PWE)	25
	2.5.2	Finite-Difference Time-Domain Numerical Method	26
CHAI	PTER 3	RESEARCH METHODOLOGY	29
3.1	Overview	N	29
3.2	Photonic	Crystal Lattice and Waveguide Structures	29
3.3	Input Se	tup	31
3.4	The Hon	nogeneous 2D Photonic Crystal	31
3.5	Photonic	Crystals Simulation by FDTD computation	33
3.6	Boundar	y Conditions	34
3.7	Periodic	Structure of the Homogeneous PhC Substrate using PWE	35
3.8	The Dire	ectional Coupler Model	38
	3.8.1	The Supercell and PBG calculation of Directional Coupler	40
	3.8.2	Coupling Length of Directional Coupler	42
3.9	Point De	fect based PCRR as WDM Filter	46
3.10	Adding l	PCRR Terminals at DC Slab	49
3.11	Spectral	Analysis	49
CHAI	PTER 4	RESULTS AND DISCUSSIONS	51
4.1	Introduc	tion	51
4.2	The Dire	ectional Coupler of the Homogeneous Si-SiO ₂ PhC	52
4.3	Point De	fect based PCRR as WDM Filter	58
4.4	PhC WD	OM Device with Directional Coupler and PCRR Terminals	62
	4.4.1	PCRR Terminals at DC Slab	62
	4.4.2	Optimization of the combined DC-PCRR PhC structure	64
CHAI	PTER 5	CONCLUSION AND FUTURE WORKS	79
5 1	Conclusi	ions	79

5.2	Recommendations for Future Works	31
REFE	RENCES	32

LIST OF FIGURES

	Page
Figure 2.1	Anderson localization, where there is a pseudo-gap present at a range of frequencies [2]9
Figure 2.2	Schematic depiction of PhCs left to right: 1-D, 2-D, 3-D [3]9
Figure 2.3	Presence of PBG in shaded area of a 1-D PhC as a multilayer film. The shaded area with PBG is the forbidden area [3]
Figure 2.4	An example gap map; of a triangular lattice PhC consisting of air holes where $\epsilon=11.4$: there are band gaps for both TE and TM modes present at different frequency ranges, and intersection of where both modes are present [3].
Figure 2.5	A schematic illustration of the basic defects on a homogeneous 2-D PhC [3]
Figure 2.6	(a) From left to right, Slab, Strip, and Fiber waveguide. Slab and Strip may be categorized together as planar waveguide [60]. (b) A 1-D PhC rib waveguide [61]
Figure 2.7	Homogeneous 2-D PhC slab with holes of lower index [69]19
Figure 2.8	(a) – (d) Hexagonal varieties of line defects employed to form various types of waveguides [50]20
Figure 2.9	Hybrid 1-D and 2-D PhC DC for WDM applications. Part I is the 1-D section and part II is the 2-D section [24]24
Figure 2.10	(a) Location of the TE fields components in the computational domain and (b) Location of the TM fields components in the computational domain. <i>Courtesy of Optiwave OptiFDTD</i> [35]28
Figure 3.1	(a) TE and (b) TM band structures as displayed by OptiFDTD of a homogeneous PhC model. The shaded area indicates the PBG where there are no bands present

Figure 3.2	The input setup in OptiFDTD. Both time and frequency domains are shown. Here the principal wavelength is at 1.55 µm. The Half width parameter defines the spectral modulation of the input31
Figure 3.3	The homogeneous 2-D PhC slab without defects consisting of Si rods on SiO_2 substrate. The lattice constant, a defines the distance between rods, where all are of the same radius in 2-D
Figure 3.4	The homogeneous 2-D PhC slab in terms of refractive indices where red indicate high index and blue low index. The range covers the refractive indices of Si and SiO ₂
Figure 3.5	Flow chart for building a PhC layout using OptiFDTD34
Figure 3.6	Boundary Condition for PEC
Figure 3.7	(a) Illustration of lattice constant, a , and rod radius, r [3]. (b) A square lattice gap map for $\varepsilon=11.4$ [3]; this is proportional to the Si-SiO ₂ pair albeit larger as it is in reference to air. Si-SiO ₂ is the practical material set in this study; (c) The band gaps of the respective ratio of the radius, r to lattice constant, a represented by r/a calculated using plane wave expansion (PWE) at working wavelengths 1.31 μ m and 1.55 μ m of materials Si and SiO ₂ [59], corresponding frequency axis is the inverse of wavelength (d) Plotted using OptiFDTD using PWE module, at $a=0.4$ μ m, the frequency region at 1.31 μ m and 1.55 μ m, r/a is 0.235
Figure 3.8	(a) PBG for Si-SiO ₂ PhC slab and (b) PBG for Si-air PhC slab38
Figure 3.9	The same homogeneous structure in Figure 3.3 with line defects applied by removing a series of single rods resulting in a gap of the width 2a
Figure 3.10	The entire PhC where two line defects are applied three rods apart, which is at two lattice constant gap 2a, along the length of the device
Figure 3.11	(a) shows the homogeneous structure where no line defects are applied and (b) with defects: size are in terms of lattice constant,

Figure 3.12	The supercell of the PhC with defect used to calculate the dispersion modes which is expected to change due to the presence of defects.	.42
Figure 3.13	Dispersion diagram of both TE and TM modes after performing PWE calculation over the supercell shown in Figure 3.12. Note the intersection with the shaded region representing the PBG of the TE modes of the homogenous PhC, this indicates mode presence in the PBG from which transfer to adjacent waveguide is possible, and from where the working coupling length is to be determined	43
Figure 3.14	(a) All TE and TM dispersion modes in PBG plotted separately.(b) Scaled curves of frequency 0.258 (1.55 μm) over k	.44
Figure 3.15	The directional coupler is defined by the coupling length as highlighted.	.46
Figure 3.16	A generic set of three PCRRs adjacent to a waveguide with the appropriate labels of the output ports	47
Figure 3.17	(a) PCRR adjacent to a single waveguide representative of the output from the DC. (b) a single PCRR where the scatter is present, and its position defined. The scatter radius is fixed for this text	48
Figure 3.18	The generic display of the PhC WDM structure consisting of DC and PCRR. The Input (Port A) is at the left where in this study is discrete at either 1.33 or 1.55. The DC section which is defined by the coupling length decides on the output waveguide of the input based on its wavelength. The 1.33 signal ought to go through the waveguide leading to Port B and 1.55 signal goes to the PCRR outputs through Channel C. Specific defects are expected to fulfill the intended WDM purpose.	49
Figure 3.19	(a) Time domain spectral distribution and (b) DFT frequency domain spectral distribution.	50
Figure 4.1	Line defects on PhC defined by the coupling length, coupling region is as highlighted.	53
Figure 4.2	Waveguide bend with single row of rods	53

Figure 4.3	Waveguide bend with two rows of rods	.54
Figure 4.4	The DC PhC with coupling region indicated by refractive index	.54
Figure 4.5	1.31 µm input propagates along the waveguide towards top output.	.55
Figure 4.6	1.55 μm input propagates along the waveguide towards bottom output.	.55
Figure 4.7	1.31 µm input propagates along the waveguide towards top output.	.56
Figure 4.8	1.55 μm input propagates along the waveguide towards bottom output.	.56
Figure 4.9	1.31 μm: Top output port of DC.	.57
Figure 4.10	1.55 μm: Bottom output port of DC	.57
Figure 4.11	A set of three PCRRs, each cavity has inner defects of 3×3 rods with respective radii, $r1$, $r2$, $r3$, of $0.7r$, $0.8r$, and $0.9r$.58
Figure 4.12	(a) The PCRRs with scatter added on the corners to form a pseudoring. (b) Details of the scatter location relative to the base PhC structure.	.59
Figure 4.13	Electrical field profile after FDTD simulation run.	.60
Figure 4.14	Output spectral distribution in time domain.	.60
Figure 4.15	Spectral distribution at the PCRR outputs, ports 1, 2, 3, respectively blue, red, green	.61
Figure 4.16	1.535 µm output at port E; note the trapped energy at the cavity before port C.	.61
Figure 4.17	1.55 μm output at port C	.62
Figure 4.18	1.57 μm output at port D	.62
Figure 4.19	Layout of the combined DC and PCRR PhC structures	.63
Figure 4.20	Spectral distribution of the combined DC and PCRR structure. Outputs' color associations are: port1 blue, port2 red, port 3 green.	.63

Figure 4.21	Continuous 1.54 µm towards output port A64
Figure 4.22	The DC model with modified layout with the ports assignment while retaining the coupling lengths
Figure 4.23	(a) to (e) are electric field, E_y transmissions and respective spectral outputs at different LC from $21a$ to $25a$ with input of $1.55~\mu m$ at Port A. Red curve represents the output at output port C and blue output Port B.
Figure 4.24	Electric field and spectral outputs when 1.31 μm input is applied at the iterations of coupling lengths 21a to 25a
Figure 4.25	Adjustments to the inter-PCRR distances, positions relative to the main bus from (a) 11a until (b) 15a
Figure 4.26	(a) to (e) spectral distributions at each PCRR-coupled output waveguide at by inter-PCRR distances 11a to 15a70
Figure 4.27	Optimized DC-PCRR PhC layout, PCRRs have uniformed layout of coupling to output waveguides
Figure 4.28	Spectral distribution at all three outputs71
Figure 4.29	Spectral output at PCRR3
Figure 4.30	Spectral output at PCRR 3 after waveguide repositioning73
Figure 4.31	Optimized DC-PCRR PhC layout, PCRRs have uniformed layout of coupling to output waveguides
Figure 4.32	Overall spectral output at PCRR ends at 30k, 50k and 150k steps with output referring to port 1, port 2 and port 3 is labelled in blue, red and green respectively
Figure 4.33	(a) isometric and (b) top view electric field and (c) spectral output at PCRR 1 with output referring to port 1, port 2 and port 3 is labelled in blue, red and green respectively
Figure 4.34	(a) isometric and (b) top view of electric field and (c) spectral output at PCRR 2 with output referring to port 1, port 2 and port 3 is labelled in blue, red and green respectively

Figure 4.35	(a) isometric and (b) top view electric field and (c) spectral output	
	at PCRR 3 with output referring to port 1, port 2 and port 3 is	
	labelled in blue, red and green respectively7	8'

LIST OF SYMBOLS

a	Lattice constant
В	Magnetic induction field
β	Propagation constant
c	Speed of light
D	Displacement field
E	Electric field
Н	Magnetic field
J	Free current density
k_e	k vector even mode
k_o	k vector odd mode
λ	Wavelength
L_B	Beat Length
L_C	Coupling Length
n	Refractive index
r	Radius
ρ	Free charge density
χ	Susceptibility tensor
ω	Frequency

LIST OF ABBREVIATIONS

ADF Add-Drop Filter

APML Anisotropic Perfectly Matched Layers

AWG Arrayed Waveguide Grating
BPM Beam Propagation Method

CWDM Coarse Wavelength Division Multiplexing

DC Directional Coupler

DFT Discretized Fourier Transform

DOS Density of States

DWDM Dense Wavelength Division Multiplexing

FBG Fiber Bragg Grating

FDTD Finite Difference Time Domain

FWHM Full Width at Half Maximum

InGaAs Indium Gallium Arsenide

GaAs Gallium Arsenide

GaN Gallium Nitride

PBG Photonic Band Gap

PCRR Photonic Crystal Ring Resonator

PEC Perfect Electric Conductor

PhC Photonic Crystal

PWE Plane Wave Expansion

Si Silicon

SiC Silicon Carbide SiO₂ Silicon Dioxide

SOI Silicon-on-Insulator

TE Transverse Electric

TM Transverse Magnetic

TIR Total Internal Reflection

WDM Wavelength Division Multiplexing

WDDM Wavelength Division Demultiplexing

PANDU GELOMBANG HABLUR FOTONIK HIBRID BERASASKAN SILIKON DENGAN KECACATAN UNTUK PENGGANDING BERARAH DAN RESONATOR CINCIN

ABSTRAK

Hablur fotonik (PhC) telah dikaji untuk integrasi litar fotonik di mana gentian optik dipertimbangkan untuk pemultipleksan pembahagian panjang gelombang (WDM) moden. Kajian ini tertumpu pada PhC sebagai calon untuk pengecilan sistem WDM. Rod silikon (Si) dua-dimensi pada silikon dioksida (SiO₂) bersama pengganding berarah (DC) dan cincin resonans PhC (PCRR) direka dan disimulasikan menggunakan OptiFDTD dengan kaedah pengembangan gelombang satah (PWE) dan perbezaan terhingga domain masa (FDTD). Peta jurang diperolehi dengan menetapkan jurang jalur fotonik pada Si-SiO₂ $0.64174 < 1/\lambda < 0.768518$ dan Si-udara 0.657996 < $1/\lambda < 0.942283$. Jarak gelombang yang dipilih merangkumi jarak gelombang komunikasi optik 1.31 μ m < λ < 1.55 μ m. Jejari rod, r dan pemalar kekisi, a, telah ditentukan pada 94.0 nm dan 0.4 µm masing-masing; r/a ialah 0.235. DC dibina dengan kecacatan malar serta input 1.31 µm dan 1.55 µm. Tiga PCRR dibina secara berasingan dengan kecacatan rongga sebagai unsur resonans. Apabila jejari rod ditetapkan pada 65.8 nm, 75.2 nm, dan 84.6 nm, DC menunjukkan input 1.31 µm dan 1.55 µm dimultipleks dalam jarak panjang gandingan 8.4 µm $< L_C < 10$ µm dan PCRR didapati menapis 1.55 µm. PCRR kemudian digabungkan pada output DC 1.55 µm dan dioptimumkan untuk mengekalkan L_C pada 8.8 µm. Output PCRR dengan jejari dalaman 0.0658 µm, 0.0752 µm, dan 0.0846 µm masing-masing adalah 1.555 µm 1.570 µm and 1.539 µm. Kajian ini menunjukkan PhC Si-SiO₂ berasaskan DC dan PCRR sesuai untuk aplikasi WDM dalam perhubungan peranti.

SILICON BASED HYBRID PHOTONIC CRYSTAL WAVEGUIDE WITH DEFECTS FOR DIRECTIONAL COUPLER AND RING RESONATORS

ABSTRACT

Photonic crystals (PhC) have been studied for photonic integrated circuits whereby optical fibres are considered for modern wavelength division multiplexing (WDM) applications. This study focuses on a PhC as candidate for miniaturization of WDM. Two-dimensional (2-D) silicon (Si) rods on silicon dioxide (SiO₂) consisting of directional coupler (DC) and PhC ring resonator (PCRR)s are designed and simulated using OptiFDTD by plane wave expansion (PWE) and finite difference time domain (FDTD). A gap map was obtained using PWE by setting the photonic band gap for Si-on-SiO₂ as $0.64174 < 1/\lambda < 0.768518$ and Si-on-air as $0.657996 < 1/\lambda <$ 0.942283. The chosen wavelengths are within optical communications wavelengths of 1.31 μ m < λ < 1.55 μ m. Rod radius, r and lattice constant, a, are determined respectively at 94.0 nm and 0.4 μ m; r/a is 0.235. A DC is built by adding line defects, decoupling 1.31 µm and 1.55 µm inputs. Three PCRRs are separately built with cavity point defects as resonator. When the rod radii is 65.8 nm, 75.2 nm, and 84.6 nm respectively, the DC demonstrated demultiplexing of 1.31 µm and 1.55 µm within range of coupling lengths 8.4 μ m $< L_C < 10 \,\mu$ m and the PCRRs demonstrated filtering over 1.55 µm. The PCRR is then combined to the DC 1.55 µm output and optimized to retain L_C at 8.8 μ m. Outputs for the three PCRRs of inner radii at 0.0658 μ m, 0.0752 μ m, and 0.0846 μ m, is 1.555 μ m 1.570 μ m and 1.539 μ m, respectively. This study shows Si-SiO₂ PhC with DC and PCRR structure can be considered for WDM applications in device interconnections.

CHAPTER 1

INTRODUCTION

1.1 Chapter Overview

This section briefly introduces the photonic crystals (PhC) and the photonic band gap phenomena associated with it, the applicability of such structures that enables wavelength division multiplexing (WDM) and demultiplexing (WDDM), and motivation for such study. Directional coupling that is used as wavelength filters in realizing WDM is introduced here as well. Included also is the concept of wavelength division multiplexing over nanoscale environment. The use of WDM in communications and inter-device interconnects is also briefly discussed. At the end of the chapter, a summary of the thesis is laid out. Throughout this thesis, light is assumed as an electromagnetic wave.

1.2 Background of Research

Periodic structure has been identified as having specific optical properties when light is propagated through it. The study on propagation of light as electromagnetic wave over periodic structure in two dimensions and more has grown since 1987 with Yablonovitch [1] and John [2] having pioneered the relatively new field of PhC at the time. Respectively, the studies were on the modification of the structures and the localization of photons in crystal lattices. The periodically structured dielectric media possesses a photonic band gap, where its length scale differ proportional to the wavelength of light. Thus, light can be controlled to be insulated, redirected, or combined, through the manipulation of the periodic structures where it propagates [3]–[5].

The capability of such periodic structure to control light opens possibilities to apply various methods of light utilization in delivering information via optical

communications. Various applications of PhC in optical communications were discussed in terms of its practical approach by Johnson et al. with emphasis on designing a slab waveguide based on PhC with importance of low crosstalk [4]. One of the applications mentioned is the combination and dispersion of light in terms of its wavelength, known as wavelength division multiplexing (WDM) [5].

An item of interest here would be the on-chip optical interconnect using WDM principles. Silicon photonics is gaining interest in research since the 2000s and especially since the 2010s, where utilising silicon as the main component for optical elements in devices is considered as one of the possible candidates for realizing highly dense WDM systems; important elements in WDM are optical multiplexers/demultiplexers, filters and switches [5].

WDM has its application in electro-optics and communications and is significantly used in fiber optics communications to distribute and combine light carriers of information over long haul networks. Since WDM is essential in a controlled delivery of light, the application ranges from the existing ones in optical telecommunications and computer networks, which has been heavily deployed, to the possible need to transfer high amount of data over short distances such as between devices within a computer system as the device [6]–[9]. The latter ventures into further miniaturization of computer components where such interconnection is an important solution where on-chip WDM applications are considered for their workability.

PhC based WDM devices or functional demonstration of such, have been investigated and demonstrated, through simulation and fabrication, in the forms of superprisms [10]–[12], coupled cavity waveguides and directional couplers, cavity waveguides, with various derivatives and combinations, all of which make use of calculated defects that appropriately act upon the waveguide.

Studies of PhC with WDM related applications were, to name a few, done by Boscolo et al [13], [14] and Martinez et al [15]–[17] regarding PhC based 2-D directional couplers and such structure was applied to a PhC based WDM system by Sharkawy et al [18], [19], Niemi et al [20] and Koshiba [21]. InAlGaAs nano-rods based PhC directional coupler was also studied [22], and the hybrid of 1-D and 2-D PhC was investigated [23], [24].

One of the reasons for the consideration of slabs is due to the significant simplicity in mapping and simulating the structure compared to the 3-D variant, which is difficult to fabricate in the real world. 2-D slabs and planar PhCs are basically structures with dielectric running in two horizontal axes where the optical field is confined in such direction, while the structure along the vertical axis's controls light through total internal reflection. The reflected light, which are traveling horizontally, are subjected to the effects of the PhC dielectric structure [4].

1.3 Problem Statement

A key component in enabling modern optical communication systems is the WDM and is realized using thin film filters known as Fiber Bragg Gratings (FBG) and arrayed waveguide gratings (AWG). Light is filtered out at specific wavelengths determined by the periodic structure of the gratings, which are basically photonic crystals, where dielectric periodicity is in one dimension.

FBGs and AWGs are effective, but problems arise when the need for closer channel spacing and smaller form factor is required. Miniaturization of the WDM elements is crucial in enabling effective optical interconnects or nanophotonic components to be practical in computers, allowing for optical based connectivity between components within the devices.

1.4 Research Motivation

Miniaturization of such device would be of great interest if it is to be employed in a chip scale environment, suitable to be used as chip or on-chip interconnection possibly for computer devices. Here it is suggested that an on-chip demultiplexer would be necessary as key component for complex multiplexing systems where physical space is limited [6]–[9], of which PhC is deemed a suitable candidate.

A key component in a WDM system is the directional coupler and was studied by Boscolo et al [13], [14]. A study was also done by Koshiba [21] where directional coupler was used as a basic building block of a WDM and WDDM. A directional coupler is demonstrated as a wavelength selective power divider [25]. Based on principles of conventional optical couplers, two waveguides that are positioned very close to each other will act as a "single" waveguide for a single light propagation. Splitting occurs when the light couples into another waveguide. Various studies have demonstrated the use of defects on PhC as a form of waveguide [13], [17], [18].

Studies on 2-D planar PhC devices have been based on the dielectric on air model where various types of optical device functionalities and their derivatives are demonstrated, and workability are also proven with fabricated PhCs for such purposes. The focus of this paper however is on the 2-D planar PhC where Si is embedded in the SiO₂ substrate where the vertical distance on the third dimension of Si from SiO₂ is not considered, having the assumption of total absence of air in the effective regions of the device, thus demonstrating the simulation of the device at lowest index difference for such combination.

In this work, a combination of two structures of PhC that are applicable to WDM systems were directional couplers and ring resonators. These two structures have been demonstrated as devices with line defect PhC directional couplers only [13]—

[18], [21]–[29] or with point defect PhC filters only [19], [20], [30]–[34]. The combination of two such structures and its optimization have not been reported, where utilisation of area on device substrate is maximized to allow a compact structure. Such line or point defects applied to a homogeneous PhC substrate enables a device to filter light by photonic band gap properties exhibited by the defected structure.

It is of interest to combine the filter structure with the directional coupler on single planar PhC where the two WDM functionalities are employed, which is the focus of the 2D design and simulation in this study. The DC acts as the main trunk of two channels with wavelengths at 1.33 µm and 1.55 µm, respectively. The 1.55 µm is further filtered to narrower wavelength spacing. When the two WDM elements are in proximity, investigating possible behaviours and limitations such as losses due to low output power and spectral shifts resulting from leakages in such structure that may emerge in a compact layout in the PhC design considerations is possible.

1.5 Scope of Simulation

The model was simulated in 2-D, such structure of the model assumed that there is no light leak over the axes outside of the plane therefore propagation of light ideally remained within the model's 2-D plane. Accordingly, the dielectric elements (rods, holes) are assumed to be very tall whereby light is confined entirely within the 2-D plane. The modeling and simulation of the PhC covers only the working region of the DC and filter and did not consider the changes of the material condition over time such as material deformation, temperature, or refractive indices variation over the mentioned conditions.

1.6 Research Objectives

The following are the research objectives:

- 1. To optimise a 2-D model of a PhC slab for WDM applications within telecommunication range of $1.33 \, \mu m$ and $1.55 \, \mu m$.
- 2. To investigate the output from multiplexing and demultiplexing activities by introducing waveguides prepared by defects within the ring resonator.

1.7 Thesis Outline

This thesis consists of five chapters. Chapter 1 is the introduction. Chapter 2 focuses on the literature reviews of this study, touching on the basic introduction to photonic crystals, its history and explanation of its fundamental theoretical foundation. Following this section, the chapter explores into the motivations for application of a PhC structure in integrated lightwave devices with attention on WDM and continue into PhC directional couplers in realizing the WDM application, and related studies involving such devices with photonic crystals as the main ingredient used.

Chapter 3 discusses on the modelling and simulation methodologies in designing a photonic crystal application in optical waveguides. Modelling touches on the concepts of the PhC directional coupler structure, its basic design and enhancements that enable its application in a WDM system, with focus on manipulations of the waveguide basic structure and consideration of a hybrid PhC. Simulation methods are also discussed with theoretical backgrounds supporting its feasibility. Also in this chapter, it covers the details of the design and simulation analyses approach of the PhC directional coupler waveguide model based on the methodologies discussed.

Chapter 4 covers the details of the design and simulation analysis of the PhC directional coupler waveguide model based on the methodologies discussed in Chapter

3. The first part focuses on the design of the directional coupler based on the base PhC set up in Chapter 3 with attention given on the performance in wavelength isolation and power retention, where wavelengths commonly used in optical communication are at 1.31 µm and 1.55 µm. The second part moves into various construction on the same base structure by introducing intra waveguide defects such as point defects and cavity defects that can extend the PhC for WDM applications. Third part of the chapter combines the structures from the first and second parts to build a simple WDM waveguide system on a PhC slab.

Chapter 5 concludes this study with suggestions for possible extension for future studies. Articles, journals, and books cited in this thesis are numbered and listed down accordingly in the reference section at the end of this thesis.

CHAPTER 2

LITERATURE REVIEW

2.1 Chapter Overview

This chapter reviews the literature related to photonic crystals and its applications in WDM, as well as various approaches that are relevant to the study conducted. This chapter starts with a theoretical background on fundamentals of a photonic crystal slab as a basic structure. Further explanation of its optical properties and the nature of light-matter interaction within the range of the optical communication transmission wavelengths of 1330 nm and 1550 nm is included.

Wavelength splitting and isolation applications are discussed with regards to its application for WDM. The needs for a WDM application at very small scale, both conceptual and practical, and the potentials for further development of photonic crystal devices is discussed. Finally, point and cavity defects are reviewed in detail with regards to its use as waveguides.

2.2 Background of Photonic Band Gap and Photonic Crystals

First notable study on electromagnetic wave on periodic media is attributed to Lord Rayleigh in 1887 [3]. Several significant milestones in the studies of electromagnetic interaction in periodic structures have since emerged. The inhibition of spontaneous emissions was studied to generalize such phenomenon for higher dimensions by Bykov [39], [40], Yablonovitch [1] and John [2], [41]. The papers described the control of spontaneous emission through creating a periodic structure that has an electromagnetic band gap forbidding spontaneous emission of photons, and of strongly localized photons producing gaps in a disordered superlattice known as the Anderson localization which is illustrated in Figure 2.1.

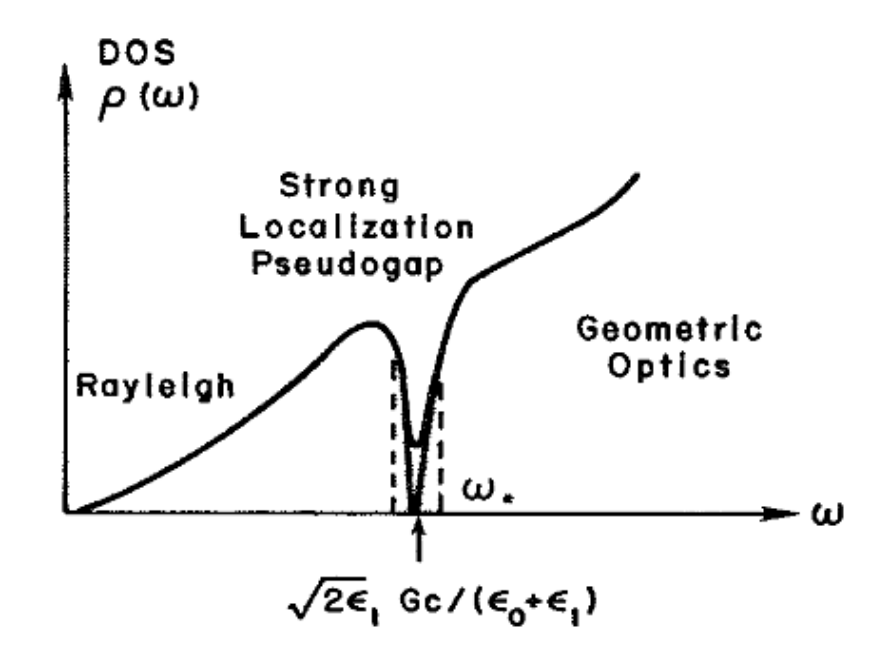


Figure 2.1 Anderson localization, where there is a pseudo-gap present at a range of frequencies [2].

A photonic crystal is a periodic dielectric medium that exhibits the photonic band gap (PBG), in which the propagation of light at certain directions with specified frequencies are prohibited, hence confining the light that falls at the same band in this PBG [3], [4]. The PBG, can be described as being analogous to the electronic counterpart with energy function of electronic band gap. The photonic crystals can be in one, two or three dimensional as illustrated in Figure 2.2.

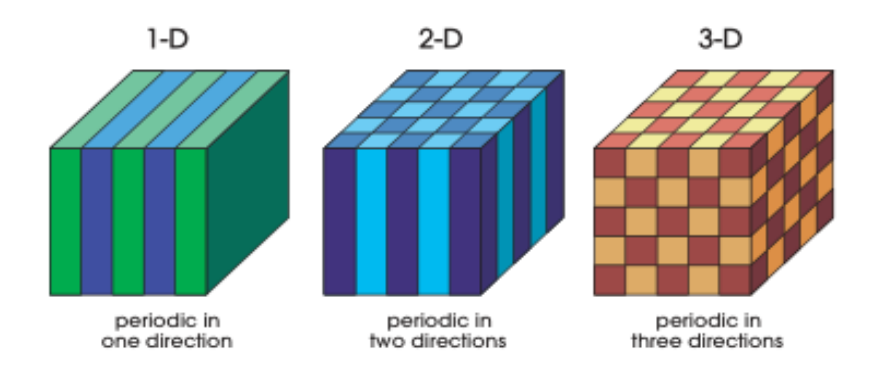


Figure 2.2 Schematic depiction of PhCs left to right: 1-D, 2-D, 3-D [3].

A one-dimensional (1-D) photonic crystal consists of periodic array of dielectric structure in one direction, be it parallel with or perpendicular to the propagation direction of light of interest. An example of 1-D photonic crystal is the distributed Bragg reflector DBR, such as the fiber Bragg grating (FBG) which has currently been largely employed in conventional optical fiber systems as a wavelength filter. Two-dimensional (2-D) photonic crystals has structures that are periodic in two axes directions over a plane, with the height axis under the plane as a homogeneous extrusion of the said plane with no complex effects on the propagation. An example of an effectively 2-D structure is the photonic crystal slab waveguide, also called planar photonic crystal. Typically, 2-D photonic crystals are in the form of periodic cylindrical rods or hollow. Three dimensional (3-D) photonic crystal, likewise, has periodicity over three axes, which is a more complex in structure as opposed to the formers. An example of a 3-D photonic crystal is the woodpile structure. Another such complex structure is known as the Yablonovite [3], [42].

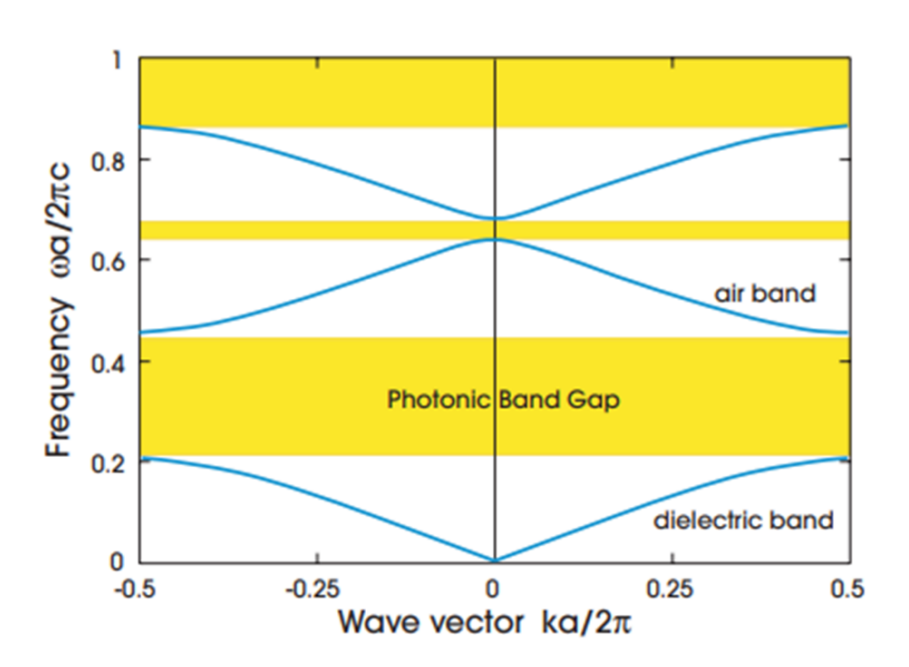


Figure 2.3 Presence of PBG in shaded area of a 1-D PhC as a multilayer film. The shaded area with PBG is the forbidden area [3].

Light propagation in periodic structures can be described in terms of Maxwell's equations as shown in eq. 1:

$$\nabla \cdot \mathbf{B} = 0$$

$$\nabla \cdot \mathbf{D} = \rho$$

$$\nabla \times \mathbf{E} + \frac{\delta \mathbf{B}}{\delta t} = 0$$

$$\nabla \times \mathbf{H} + \frac{\delta \mathbf{D}}{\delta t} = \mathbf{J}$$
(1)

where **E** is the macroscopic electric field, **H** the macroscopic magnetic field, **D** is the displacement field, and **B** is the magnetic induction field; ρ and **J** is the free charge density and the free current density, respectively. Taking the component D_i from the displacement field **D** and relate to the component E_i of electric field **E**, by non-linear power series [3], [43], the following equation is formed:

$$D_i/\varepsilon_0 = \varepsilon(\mathbf{r}, \omega)E_i + \sum_{j,k} \chi_{ijk} E_j E_k + O(E^3)$$
(2)

where ε_0 is the electric permittivity in vacuum given by the constant value of approximate 8.854×10^{-12} Farad/m and χ is the susceptibility tensor, and higher orders are in the terms in $O(E^3)$. In many cases for dielectric materials, it is assumed that when field strengths are small in the linear regime, the χ_{ijk} is ignored. As the material being macroscopic and isotropic, $\mathbf{E}(\mathbf{r},\omega)$ and $\mathbf{D}(\mathbf{r},\omega)$ are related by the relative permittivity, ε , which is ε_0 multiplied by $\varepsilon(\mathbf{r},\omega)$.

Having the propagation without the source of light, where $\rho=0$ and J=0, simplifies the Maxwell in **E** and **H** terms equation to:

$$\nabla \cdot [\varepsilon(\mathbf{r})\mathbf{E}(\mathbf{r},t)] = 0 \qquad \nabla \times \mathbf{E}(\mathbf{r},t) + \mu_0[\delta \mathbf{H}(\mathbf{r},t)/\delta t] = 0$$

$$\nabla \cdot \mathbf{H}(\mathbf{r},t) = 0 \qquad \nabla \times H(\mathbf{r},t) - \varepsilon_0 \varepsilon(\mathbf{r})[\delta \mathbf{E}(\mathbf{r},t)/\delta t] = 0$$
(3)

where ε_0 and μ_0 is the electric permittivity and magnetic permeability constants, respectively, in vacuum. From here it can be derived as follows:

$$\mathbf{H}(\mathbf{r},t) = \mathbf{H}(\mathbf{r})e^{-i\omega t} \qquad \mathbf{E}(\mathbf{r},t) = \mathbf{E}(\mathbf{r})e^{-i\omega t}$$
(4)

Inserting the equations in 4 into 3,

$$\nabla \cdot \mathbf{H}(\mathbf{r}) = 0 \qquad \qquad \nabla \cdot [\varepsilon(\mathbf{r})\mathbf{E}(\mathbf{r})] = 0$$
 (5)

Relating the two curl equations to $\mathbf{E}(\mathbf{r})$ and $\mathbf{H}(\mathbf{r})$:

$$\nabla \times \mathbf{E}(\mathbf{r}) - i\omega \mu_0 \mathbf{H}(\mathbf{r}) = 0 \qquad \qquad \nabla \times \mathbf{H}(\mathbf{r}) - i\omega \varepsilon_0 \varepsilon(\mathbf{r}) \mathbf{E}(\mathbf{r}) = 0$$
(6)

The following is called the master equation in terms of $\mathbf{H}(\mathbf{r})$, which is useful in performing numerical computations:

$$\nabla \times \left(\frac{1}{\varepsilon(\mathbf{r})} \nabla \times \mathbf{H}(\mathbf{r})\right) = \left(\frac{\omega}{c}\right)^2 \mathbf{H}(\mathbf{r})$$
(7)

where c is speed of light in vacuum. In the master equation the $\mathbf{H}(\mathbf{r})$ can be solved.

Eq. 8 shows the corresponding electric field $\mathbf{E}(\mathbf{r})$ component based on eq. 6.

$$\mathbf{E}(\mathbf{r}) = \frac{i}{\omega \varepsilon_0 \varepsilon(r)} \nabla \times \mathbf{H}(\mathbf{r})$$
(8)

For a given structure $\varepsilon(\mathbf{r})$, solving the eq. 7 and 8 by numerical computation, the $\mathbf{E}(\mathbf{r})$ and $\mathbf{H}(\mathbf{r})$ can be profiled and mapped to a PhC.

2.3 Base Photonic Crystal Structure

2.3.1 Substrate Materials and Layout

Optical devices have been based on the III-V group and on silicon as base. As silicon-based microprocessors are approaching its physical limit [44], a PhC structure may be considered for employing on-chip solutions [6]–[8].

Silicon-based PhCs in macroporous form consisting of holes were demonstrated whereby a simple waveguide was formed by a line defect [45]–[47]. Silicon pillars in the forms of rod were also demonstrated prepared by electrochemical etching and oxidation of microporous silicon [48]. SiO₂-Si-SiO₂ sandwich structure of PhC slab waveguide is demonstrated by drilling holes to make a 2-D PhC [49], [50]. Silicon Carbide (SiC) of which the hardness of the material was being considered, have been fabricated effectively producing 40 nm bandwidth waveguide [51].

The materials of interest here are silicon based, two of which are Si and SiO₂ being typical in the semiconductor industry [52], [53]. The high index contrast between the two materials enables more potential for control over the propagation as a waveguide. Such index difference has been treated as Si floating in air of which the refractive index is at 1.00 thus maximizing the effective refractive index. Such a condition allows for the largest band gap to be possible for any one material pairing. A structure where the Si element that is embedded in the SiO₂ is demonstrated as a waveguide formed by line defects [54]. The demultiplexer structure in [33] is similar to the embedded type, as both are consisted of a simple set of point defects adjacent to a main bus waveguide as wavelength filters. Refractive indices of Si and SiO₂ used for the design and simulation of the 2-D PhC are $n_{\rm Si} = 3.4757$ and $n_{\rm SiO_2} = 1.444$ [55], respectively.

2.3.2 The Gap Map

A convenient way to design a general PhC is by using a reference tool called "Gap Map" [56]–[58], where in its general form is a plotted graph of lattice constant over wavelength, a/λ vs radius per lattice constant, r/a. The area of the graph indicates the band gaps. The wavelength of the light source in frequency is defined and from there the radial structure of the PhC basic cell is obtained. Additionally, the lattice constant is determined which leads to the final design with finite edges. Note that the presence of lattice constant in both parameters of the gap map, is the representative of the scalable property of PhC, and is necessary to obtain the suitable lattice constant of any PhC by defining the wavelength range of interest [3]. Further explanation of this approach is in Chapter 3.

The Gap Map have been applied to both triangular periods and rectangular periods, and to rods and holes structures [57] and such would be the first reference as a foundation of any PhC design. Plotting the gap map enables a limited degree of analytical approach of designing the PhC where the lattice constant, a, and the ratio of periodic radius-to-lattice constant, r/a are defined in progression of the design of the waveguide system. Consideration of parameters used for this approach does appear to be rather simple, where the wavelength is first determined, and gap map plotting is used to obtain the periodic ratios from which the structure takes shape. An example of the gap map is shown in Figure 2.4 which is a representative of simple possibilities of band gap types present in a PhC.

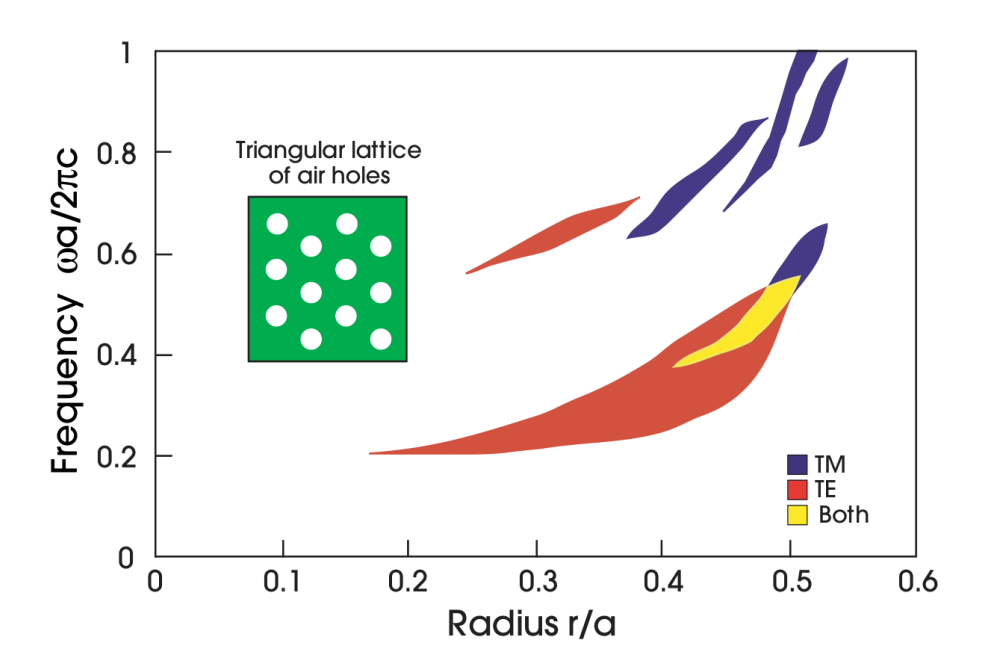


Figure 2.4 An example gap map; of a triangular lattice PhC consisting of air holes where $\varepsilon = 11.4$: there are band gaps for both TE and TM modes present at different frequency ranges, and intersection of where both modes are present [3].

It is noted that the gap maps are classified by a single material over air. Effective refractive index determines the distribution of the gap map plotting that will be useful for the Si-SiO₂ material where a gap map is plotted in [59].

2.4 Photonic Crystal Defects

A defect is described as a deliberate application of irregularity on an otherwise geometrically and materially homogeneous periodic structure for a specific design purpose [3], [5]. Such defects can be in the form of point; a single unit of basic element of the periodic structure, or line; a continuous series of points. The defect can be in the form of absence of the unit element, or difference in the unit element geometry, and refractive index, examples of common approaches.

By having defects where series of points are removed from a homogeneous lattice, a guide is formed for electromagnetic waves to be within a confined propagation through the PhC. The defects are typically in the form of linear and point defects on a homogeneous PhC. The point defect is applicable in the formation of a

cavity filter while the linear defect is in the formation of waveguide [3], as shown in figure 2.5.

A design of a simple light manipulating device can be made with a photonic crystal by applying the defect, from as simple as a single element defect of either line or point, to a more complex multiples of such elements with calculated and analysed positioning, or even hybrid forms of which there are combination of different elements or dimensional properties (be it of 1-D, 2-D or 3-D). Such structure can be simulated by plane wave expansion (PWE) and finite-difference time domain (FDTD) methods, of which are to be visited at the end of this chapter. The typical types of PhC applications based on the described defects are explored in the following sections.

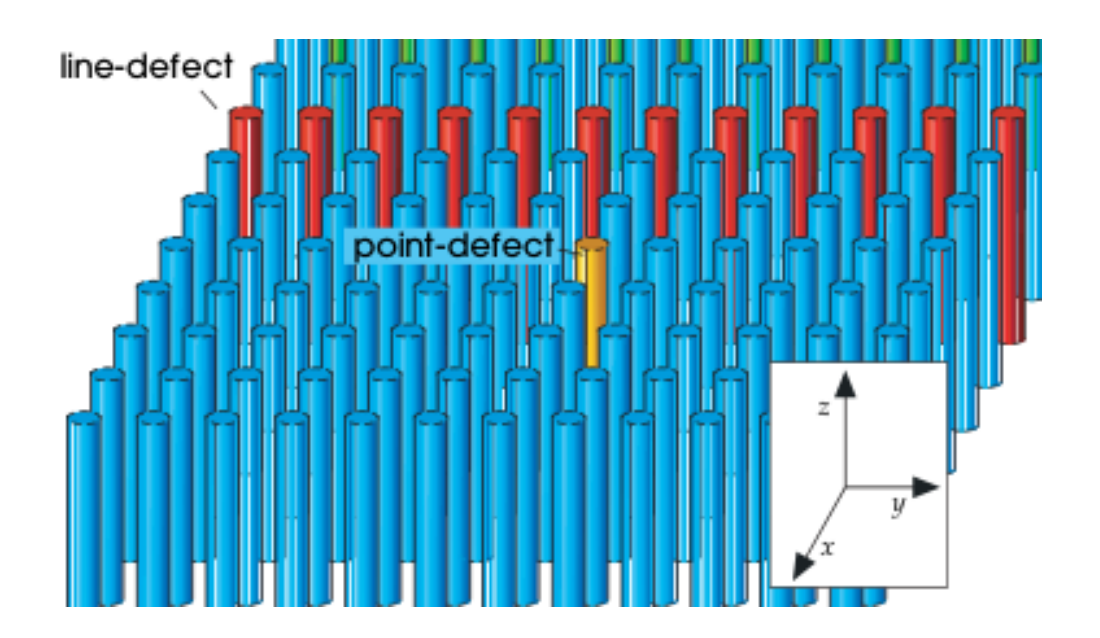


Figure 2.5 A schematic illustration of the basic defects on a homogeneous 2-D PhC [3].

2.4.1 Photonic Crystal Slab Waveguide

A waveguide guides light as an electromagnetic wave, and an optical waveguide guides light within the optical spectrum. Traditionally, an optical waveguide is based on total internal reflection (TIR) where light is confined through

difference in reflective index as governed by Snell's Law where a terminal propagation angle would result in light reflecting back repeatedly into the lower refractive index medium of the waveguide. This can be referred to as index guiding, the interfacing of high-index medium and low-index medium. Optical waveguide comes in the following geometrical forms: fiber, strip, and planar waveguide in the form of a slab as shown in Figure 2.6 (a) [60].

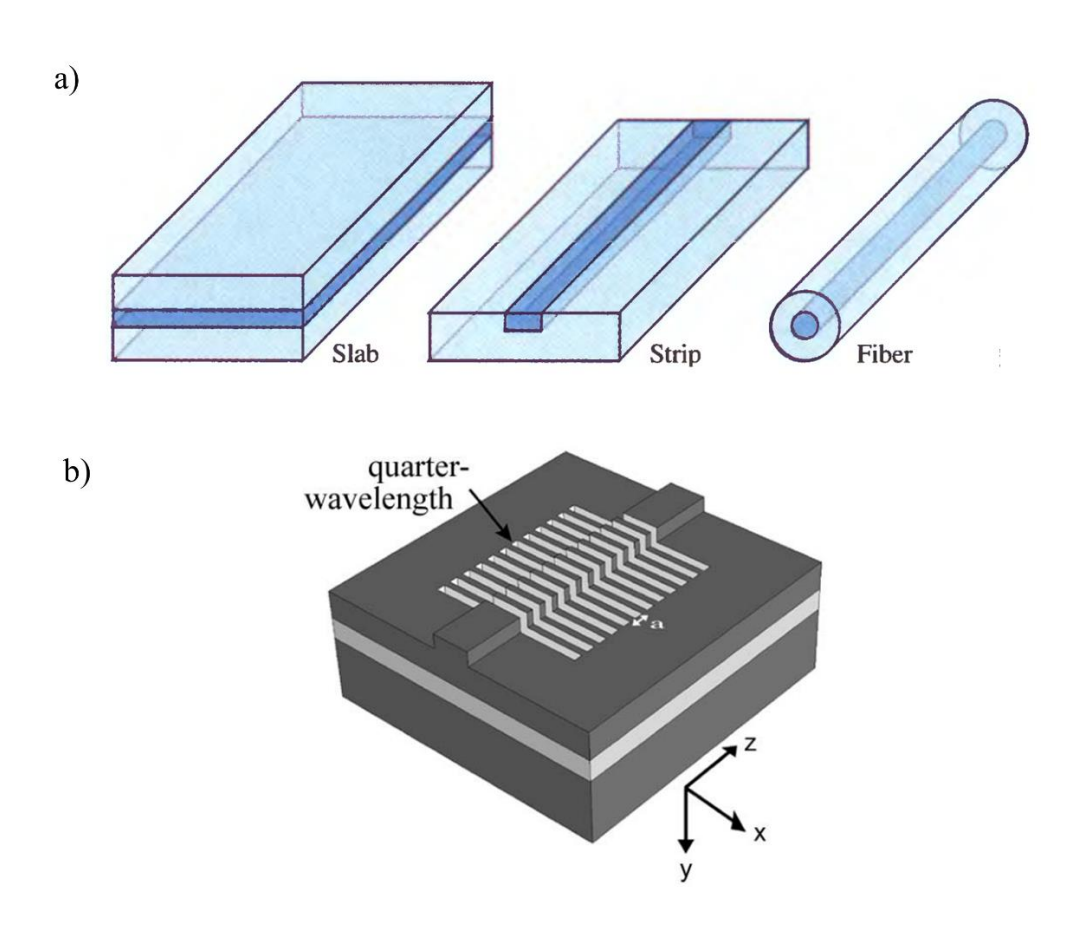


Figure 2.6 (a) From left to right, Slab, Strip, and Fiber waveguide. Slab and Strip may be categorized together as planar waveguide [60]. (b) A 1-D PhC rib waveguide [61].

In optical communications, a waveguide is the basic structure of photonic devices in guiding, coupling, switching, splitting, multiplexing, and demultiplexing of light. Therefore, it is a key element in any photonic integrated circuits, where the mentioned applications are the elements of a photonic circuit in manipulating light.

Some examples of 1-D PhC waveguides were demonstrated as a rib waveguide, as shown in Figure 2.6 (b) [61]. This waveguide has light propagation perpendicular to the periodicity of the structure. Examples of the ID waveguides are anti-resonant reflecting optical waveguide with hollow cores [62], light splitting structure where transfer occurred over two parallel waveguides [63], and as part of a hybrid structure for improved light confinement and coupling [24].

In a two-dimensional (2-D) PhC, a waveguide is formed by having a line defect applied across the periodic structure. As any point defect will confine light of a specific range of wavelengths, if there is a PBG corresponding to it, a series of such defects will form a line that guides the light with no scattering on the surrounding periodic structure.

WDM requires an effective method in propagating light while preserving the properties of the light. An important element widely used for WDM applications is an optical directional coupler (DC). To have such a system operating within a scaled down photonic integrated circuit, PhC is an excellent candidate. It has been experimentally proven that designing couplers based on PhC is possible [19] [13]–[18], [21], [22], [24]–[29].

The slab structure has been studied extensively and widely [49], [58], [64]–[68] and is proposed as the fundamental building block for future PhC based optical systems, where slab parameters such as thickness [68] is studied. The key reason is the facility of design where the PBG is obtained at 2-D plane while the vertical confinement is reduced to only applying refractive index difference on the cladding-substrate structures [49], [64], [65].

PhC waveguide has largely been studied whereby the PhC is floating in air to maximize the effective refractive index difference. However, a practical condition

ought to be considered as demonstrated by Yamada (NTT) in the study of Silicon-on-Insulator (SOI) PhC waveguides [69]. The structure used in this study was a hole based PhC slab constructed on a SOI substrate. Illustration from the research work is shown in Figure 2.7 whereby the waveguide was formed on the 2-D surface of a slab structure by a single row of line defect for light propagation. The fabrication shows periodic holes etched through the Silicon (Si) layer on top of Silicon Dioxide (SiO₂).

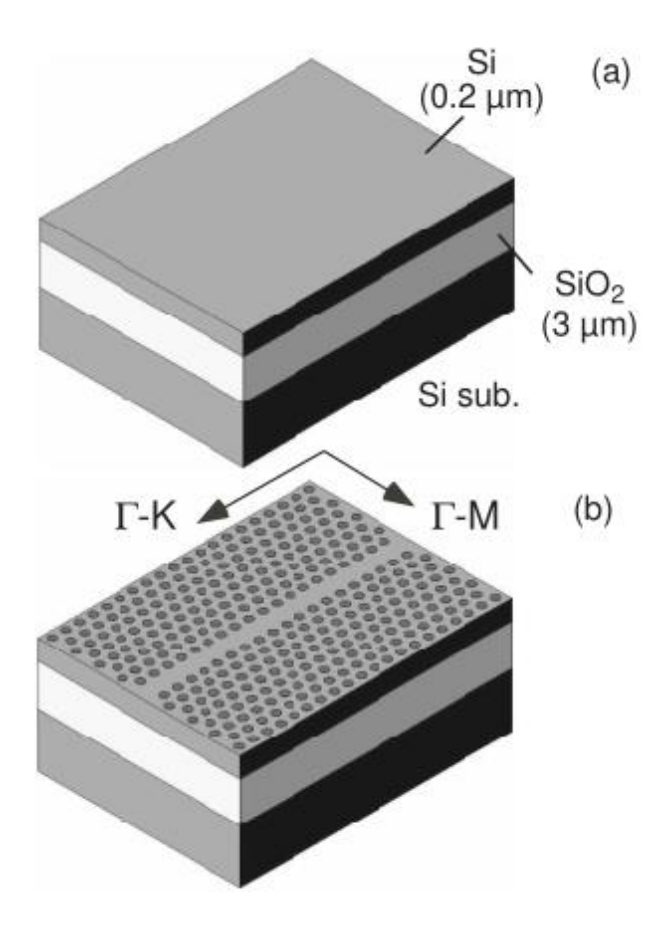


Figure 2.7 Homogeneous 2-D PhC slab with holes of lower index [69].

A waveguide on the PhC is formed by applying series of point defects over the periodic structure where the affected region breaks the periodicity. SOI based 2-D PhC slab with changes of the applied line defect as a waveguide is shown in Figure 2.8.

The waveguide was fabricated from the holes through SiO₂ cladding and the Si core in hexagonal lattice form [50].

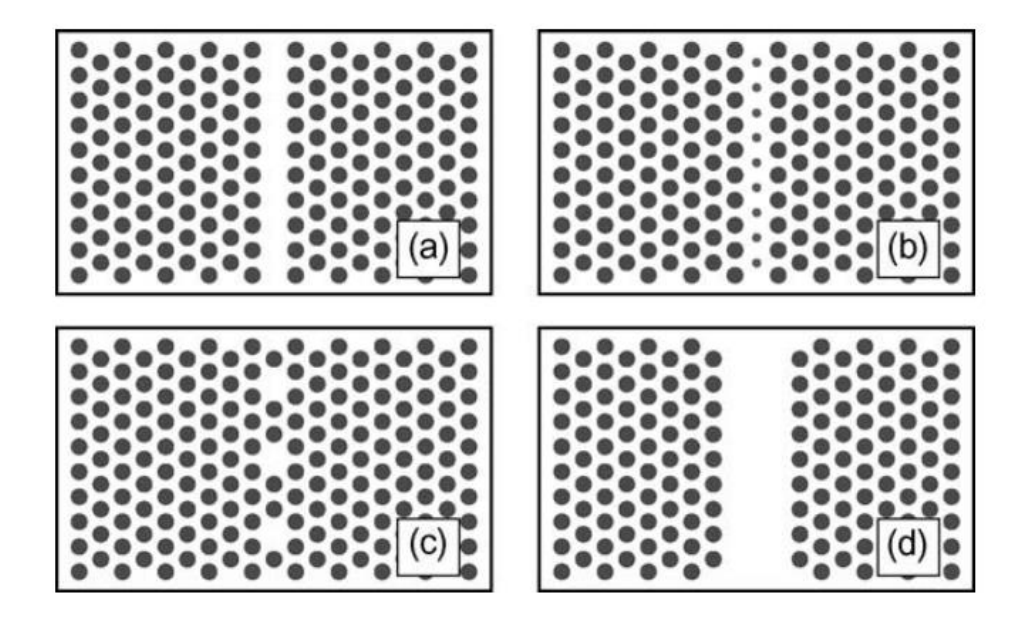


Figure 2.8 (a) - (d) Hexagonal varieties of line defects employed to form various types of waveguides [50].

There is also a consideration on the width of the waveguide (cross sectional aperture) whereby a line defect is defined in terms of the lattice constant, *a*. Yamada et al came up with a 1.182*a* line defect on a PhC structure with fixed *a* for the periodic lattices surrounding it. Defect width variations may also break the lattice constant throughout the homogeneous base of a PhC waveguiding structure [69]. Niemi et al Click or tap here to enter text.demonstrated a working WDM filter structure of demultiplexing at sub nm wavelengths using point defects where the sizes are manipulated [20]. Such defect has been shown to work for small wavelength filtering [15], [19], [20], [31], [33], [70]–[76].

2.4.2 Directional Coupler for WDM by Line Defects

WDM is the division and combination of light, which includes both splitting (demultiplexing) and combining (multiplexing). In this literature, WDM specifically

refers to both. Important properties that enable effective coupling are the coupling coefficient and the coupling length. Therefore, an effective coupler is able to couple light of different wavelengths while preserving its power at the output end of the coupler, at shortest possible distance contributing to the overall size of the directional coupler. From [13], [14], the coupling length is expressed in terms of even and odd wavevectors where it is defined as half of beat length, L_B :

$$L_C = \frac{\pi}{|\beta_e - \beta_o|} = \frac{1}{2} L_B \tag{9}$$

Where L_B is the beat length and β is the propagation constant. Here, the β is subscripted with even and odd modes. The difference of the β is obtained by identifying the state at the output region difference to input in terms of wavevector k, β is expressed for both even and odd modes, β_e and β_o respectively as [77]:

$$\beta_e = \frac{2\pi \times k_e}{a}$$

$$\beta_o = \frac{2\pi \times k_o}{a}$$
(10)

The Coupling length, of which is twice the beat length which is $L_C = 2L_B$ is expressed in wavevector terms as follows:

$$L_{C} = \frac{2\pi}{|k_{e} - k_{o}|}$$

$$|\kappa| = |k_{e} - k_{o}| = \Delta k$$

$$L_{C} = \frac{\alpha}{2|\kappa|} = \frac{\alpha}{2\Delta k}$$

$$L_{C} = \frac{\pi}{|\Delta \kappa|}$$
(11)

Extensive studies on directional couplers were performed by Koshiba *et al* using PhC MUX-DEMUX waveguide of square lattice floating on air [21]. Simulation was done using beam propagation method (BPM). The study showed that a MUX-DEMUX device can be drastically reduced to a few hundred micrometers with capability of managing channel spacing of 20 nm as required for wide-passband WDM (WWDM) systems. The coupling length demonstrated was at range of 23a to 36a, rod size of r = 0.18a and n = 3.4 [55].

Boscolo *et al.* demonstrated coupling and decoupling of electromagnetic waves in parallel 2D PhC [13], [14] of two nearby straight PhC waveguides, in which energy transfer is achievable by accurately calculating the coupling length through the analysis of the dispersion modes that exists in the PBG of the PhC defect structure.

Martinez *et al* has introduced a design for ultrashort directional couplers [15]—[17], whereby the coupling length can be shortened with increasing coupling coefficient on a 2-D PhC. The coupling coefficient can be increased by having a set of two parallel PhC waveguides based on line defect in the form of single empty row of removed rods separated by a reduced size radius of PhC of similar lattice constant to the general structure. This results in a small interleaver applicable for wavelength demultiplexer.

Effects on the PhC directional coupler effectiveness was investigated whereby the lattice structure profile plays a role in the effective coupling length while satisfying the controlled design outcome of the coupling coefficient of the PhC structure [28], [29]. It is also observed that coupling length reduces as incident wavelengths increase.

2.4.3 Cavity Filter for WDM by Point Defects

Components in an optical device for WDM system may include channel add/drop filters (ADF). In a PhC, resonant cavities can be formed by employing point defects.

The coupling of waveguides interfaced by such defects were achieved through the introduction of a cavity defect within the vicinity of the coupled region [15], [31], [78].

To form a resonant cavity, the point defects on PhC need to be employed in various manners. One manner is by removing a PhC element such as rod or hole from the homogeneous structure, or by changing a certain part of the PhC structure where the cavity is intended in terms of material types, size, or shape of the element. PhC channel drop filters [30], [70] in its general form is discussed and demonstrated where full transfer between two waveguides is possible with resonant states of different symmetry, by forcing an accidental degeneracy.

In PhC Ring Resonators (PCRR), in which the circularity in the resonant cavity can be employed in various forms, such as displaced rods and holes from the homogeneous PhC to build a circle and the use of scatter to effectively produce spatial effect of a ring waveguide acting as a resonator [34], [79]. Simple single point cavities [19], [20], [31], [33], [76] and complex [80] structures have been studied where various wavelength specific filtering were achieved but maintaining high degree of quality factor, indicating successful employment of the resonant cavity in the PhC. The structures are designed and simulated with the high index elements being in air, where such element is very far from low index substrate material its refractive index may be negligible. Furthermore, more recent studies were done such as the employment of a nanobeam PhC cavities where further miniaturization was predicted.

2.4.4 Hybrid PhC Structures

A hybrid PhC is a combination of different topologies on a single working device. This can be in the form of combining a 1-D, 2-D, and even 3-D PhCs in each permutation, where typically would be in the 1-D and 2-D, or combination of defects forming respective subsystems within a single defined device.

An example is shown in Figure 2.9 as demonstrated by Hanapiah et al [24]. The 1-D section of linear waveguides parallel to the propagation of light works in enhancing signal quality prior to the 2-D region where coupling/decoupling occurs within such system.

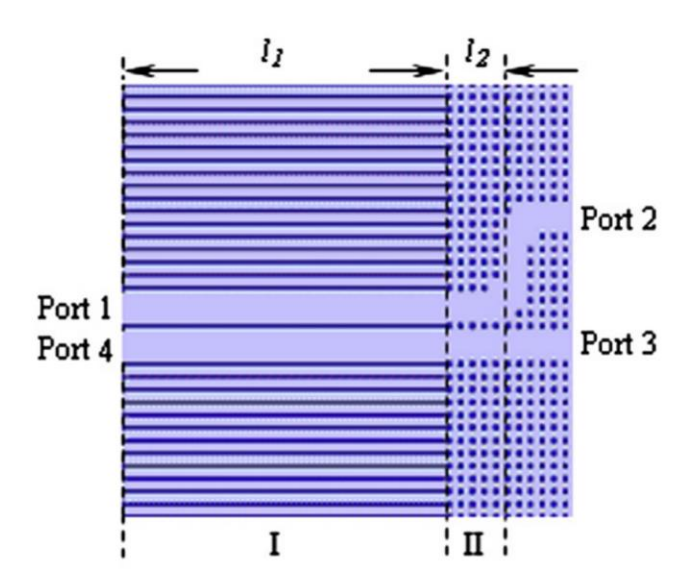


Figure 2.9 Hybrid 1-D and 2-D PhC DC for WDM applications. Part I is the 1-D section and part II is the 2-D section [24].

Line defect and point defect structures have been demonstrated individually. The combination of two such structures in a single device and its optimization is yet to be studied.

In this thesis, the focus is the hybrid of a line-defect based component being the DC and another component being the PCRR, whereby different refractive index material are used when point or line defects is absent with the added benefit to simplify for mass fabrication.

2.5 Simulation Methods

Two numerical methods were considered here, the Plane-wave Expansion (PWE) and the finite-difference time-domain (FDTD) method. Both methods were employed in the same tool [35] where information and its conventions are explained